Dynamics of anisotropic Rényi holographic dark energy model

Y. Aditya
Department of Mathematics, GMR Institute of Technology, Rajam-532127, India
aditya.y@gmrit.edu.in; yaditya2@gmail.com
(Submitted on 5 September 2023; Accepted on 23 November 2023)

Abstract. In the background of the Saez-Ballester (Saez and Ballester 1986) theory of gravitation, the manuscript presents the study of Rényi holographic dark energy determined through interaction and non-interaction in the anisotropic and spatially homogeneous Bianchi type-I space-time. We determine both non-interacting and interacting dark energy models by considering a correlation between the metric potentials to solve the field equations of the model. This results in a dynamical deceleration parameter which demonstrates a shift in the cosmic rate of acceleration from deceleration to acceleration, with a redshift z change that is compatible with observations. Despite assuming several values to parameters ω_{de} close to -1 at $z=0$ (the present epoch) and being in agreement with the most recent observations, the equation of state parameter ω_{de} for the two Rényi holographic dark energy models displays substantially different dynamic behaviour. Next, we discovered that the squared sound speed, v_s^2, is negative, implying instability against perturbations. The ω_{de}-ω_{de}' plane is constructed to investigate the evolution of the models' EoS parameter turned out to be in a zone of freezing. As should be the case in an expanding universe, the strong energy conditions of the models are violated. Our models include the Chaplygin gas, ΛCDM limit, and are inclined towards the steady-state model. Statefinders (r, s), and $r-q$ planes were also examined.

Key words: Saez-Ballester theory of gravity, Bianchi type model, Rényi holographic dark energy, Cosmology, Dark energy.

1 Introduction

Cosmic acceleration is supposed to occur in our universe. The reason for this is believed to be dark energy (DE), a mystery type of energy with extremely high negative pressure. Different cosmological observations (Riess et al. 1998; Perlmutter et al. 1999; Spergel et al. 2003; Tegmark et al. 2004) have demonstrated the existence of this kind of energy. Its precise nature, however, is still an unresolved issue that requires additional research. The cosmological constant is the first and most simple option for DE, however, it has two significant theoretical problems, including coincidence and fine-tuning problems. In order to address the DE problem, two approaches have been suggested: one involves studying the dynamics of numerous DE models, and the other involves modifying the Einstein-Hilbert action of the general theory of relativity, which results in modified theories of gravity. Using the variable equation of state (EoS) parameter $\omega_{de}=p_{de}/\rho_{de}$ (p_{de} is the pressure and ρ_{de} is the energy density of DE), the DE models may be divided from the cosmological constant. The familiar DE models are scalar field models which include quintessence, phantom, quintom, etc. (Padmanabham 2002, 2008; Bento et al. 2002; Caldwell 2002; Nojiri and Odintsov 2003a) and the DE models which contain a family of Chaplygin gas, agegraphic DE models, holographic DE (HDE), etc. (Kamenshchik et al. 2001; Bento et al. 2002; Sahni and Shtanov 2003; Hsu 2004; Cai 2007).

Among several dynamical DE models, HDE is attracting several researchers in this field. HDE is based on the well-known holographic principle (Hooft 1993; Cohen et al. 1999; Susskind 1995). This principle creates an upper bound

for the universe's entropy in a cosmic framework, and there is a theoretic interaction between ultraviolet (UV) and infrared (IR) cutoffs. The energy density ρ_{de} in a region associated with the UV can be obtained from

$$L^3\rho_{de} \leq LM_p^2. \tag{1}$$

The relation described in Eq. (1) can be used to determine the maximum value of L in this instance, where the energy density of HDE is given by

$$\rho_{de}= 3c^2M_p^2L^{-2}. \tag{2}$$

In this equation, M_p^{-2} is the reduced Planck mass, $M_p^{-2}= 8\pi G$, and c is a numerical constant. Any modification to the area law of entropy, upon which the energy density of the HDE is based, results in a modified holographic energy density. More recently, the Tsallis HDE (THDE) (Tsallis and Cirto 2013; Tavayef et al. 2018), Sharma-Mittal HDE (SMHDE) (Jahromi et al. 2018), and Rényi HDE model (RHDE) (Moradpour et al. 2018a) entropy formalisms have been used to construct HDE models. There have been discussions of the SMHDE, THDE and RHDE cosmological models in the Chern-Simons theory of gravity in the contexts of the D-dimensional fractal universe, the DGP braneworld (Younas et al. 2019; Maity and Debnath 2019; Iqbal and Jawad 2019). Prasanthi and Aditya (2020, 2021), Aditya et al. (2019) and Bhattacharjee (2020) have investigated the observational constraints on the RHDE and THDE models. In addition to using three distinct parametrizations of the interaction between dark sectors (dark matter and DE), Sharma and Dubey (2022) examined RHDE in a flat isotropic universe where the Hubble horizon serves as the IR cut-off. The RHDE model with the particle and future horizons as the IR cut-off has been studied by Chunlen and Rangdee (2021). RHDE in Ruban's Universe has been investigated by Santhi and Chinnappalanaidu (2022), where Hubble Horizon takes care of the IR cutoff.

The study of modified theories of gravitation (such as Brans-Dicke (1961), Saez-Ballester (SB) (1986) scalar-tensor theories, $f(R)$ (Nojiri and Odintsov 2003b) and $f(R,T)$ (Harko et al. 2011) theories, where R is the curvature scalar and T is the trace of the energy-momentum tensor) is significant to explain the DE models. The literature on the subject provides a comprehensive examination of DE models as well as modified theories of gravity (Copeland et al. 2006; Setare 2007; Clifton et al. 2012; Bamba et al. 2012; Nojiri et al. 2017). The metric potentials and a dimensionless scalar field are connected in the SB theory of gravity. They have demonstrated that the weak fields are effectively described by this minimal coupling. The SB field equations are provided by

$$R_{ij} - \frac{1}{2}Rg_{ij} - w\phi^n\left(\phi_{,i}\phi_{,j} - \frac{1}{2}g_{ij}\phi_{,k}\phi^{,k}\right) = -\frac{8\pi G}{c^4}T_{ij} \tag{3}$$

and the scalar field ϕ satisfies the equation

$$2\phi^n\phi^{;i}_{;i} + n\phi^{n-1}\phi_{,k}\phi^{,k}= 0 \tag{4}$$

where w is a dimensionless constant, G is the gravitational constant, T_{ij} is the stress-energy tensor of the matter, and semicolons and commas indicate covariant and partial differentiation, respectively. The following is the energy-conservation equation:

$$T^{ij}_{;j} = 0. \tag{5}$$

The observable universe is almost homogenous and isotropic, as is well known. As a result, cosmology has given the FRW models a lot of attention. However, the fact that there were only a few anisotropies in the universe's early history prompts us to think of homogenous anisotropic Bianchi type (BT) models. Specifically, the BT-I model, which represents a spatially homogenous, anisotropic, and flat universe, is considered to be the basic anisotropic universe model. To address the significance of anisotropies in the universe, several authors have recently been looking into anisotropic BT models in the presence of several matter distributions. As analyzed in detail by Quiros and Rangel (2023), the SB theory is in fact Einstein theory of gravity with minimally coupled mass-less scalar field. The BT-I generalized ghost pilgrim DE model has been examined by Santhi et al. (2017a). In SB's theory of gravitation, BT-I and III modified holographic Ricci DE (MHRDE) have been studied by Rao and Prasanthi (2017). The BT- VI_0 MHRDE cosmological model in the SB theory of gravity has been addressed by Santhi et al. (2017b). BT-V DE model with cosmic strings has been examined by Mishra et al. (2018). In the background of the $f(R)$ gravity, Aditya and Reddy (2018a) studied the BT-I string cosmological models, whereas Sharif et al. (2018) studied the BT-I new HDE model. In scalar-tensor theories of gravity, Santhi and Appalanaidu (2023) have examined several THDE models of the BT universe. The anisotropic RHDE model in the SB theory of gravity has been explored by Vinutha et al. (2023). Aditya (2023) and Aditya and Prasanthi (2023) have studied anisotropic dark energy models in modified theories of gravitation.

In this study, inspired by the previous discussion, we investigate the locally rotationally symmetric (LRS) BT -I RHDE model in SB theory of gravitation. The following describes the way the paper is structured: In Section 2, we derive the model's field equations and solve them to describe non-interacting and interacting models. In this section various physical features of the models are also included. In Section 3, we compare our study to recent research works on the subject and modern observational data. Section 3 also includes a summary of the results obtained.

2 Field equations and models

Anisotropic LRS Bianchi type-I space-time is considered as

$$ds^2 = dt^2 - A^2(t)dx^2 - B^2(t)[dy^2 + dz^2] \tag{6}$$

where A and B are metric potentials and solely functions of cosmic time t. The physical parameters for the LRS BT-I model are defined as follows:
Mean Hubble's parameter

$$H = \frac{\dot{a}}{a} = \frac{1}{3}\left(\frac{\dot{A}}{A} + 2\frac{\dot{B}}{B}\right) \tag{7}$$

where $a(t) = (AB^2)^{1/3}$ is the average scale factor. Expansion and shear scalars are, respectively, defined as

$$\theta = u^i_{;i} = \frac{2\dot{A}}{A} + \frac{\dot{B}}{B} \tag{8}$$

$$\sigma^2 = \frac{1}{2}\sigma^{ij}\sigma_{ij} = \frac{1}{3}\left(\frac{\dot{A}}{A} - \frac{\dot{B}}{B}\right)^2. \tag{9}$$

The SB field equations for DE and matter distribution are provided by (with $8\pi G = 1$ and $c = 1$)

$$R_{ij} - \frac{1}{2}g_{ij}R - \omega\phi^n(\phi_{,i}\phi_{,j} - \frac{1}{2}g_{ij}\phi_{,k}\phi^{,k}) = -(T_{ij} + \overline{T}_{ij}), \tag{10}$$

where T_{ij} and $\overline{T}_{ij}$ are the matter and DE energy-momentum tensors, respectively. The scalar field satisfies the equation

$$2\phi^n\phi^{;i}_{;i} + n\phi^{n-1}\phi_{,k}\phi^{,k} = 0, \tag{11}$$

and energy-conservation equation is defined as

$$\overline{T}^{ij}_{;j} + T^{ij}_{;j} = 0. \tag{12}$$

The energy-momentum tensors for matter T_{ij} and anisotropic DE $\overline{T}_{ij}$ are given by

$$T_{ij} = diag[1, 0, 0, 0]\rho_m$$

$$\overline{T}_{ij} = [1, -\omega_{de}, -(\omega_{de} + \gamma), -(\omega_{de} + \gamma)]\rho_{de} \tag{13}$$

where ρ_m and ρ_{de} are the energy densities of matter and DE, $\omega_{de} = \frac{p_{de}}{\rho_{de}}$ is the EoS parameter and skewness parameter γ is the deviation from EoS ω_{de} on y and z axes.

With the use of (13), the field Eqs. (10)-(12), for metric (6), may be represented as

$$2\frac{\ddot{B}}{B} + \frac{\dot{B}^2}{B^2} - \frac{w}{2}\phi^n\dot{\phi}^2 = -\omega_{de}\rho_{de} \tag{14}$$

$$\frac{\ddot{A}}{A} + \frac{\ddot{B}}{B} + \frac{\dot{A}\dot{B}}{AB} - \frac{w}{2}\phi^n\dot{\phi}^2 = -(\omega_{de} + \gamma)\rho_{de} \tag{15}$$

$$2\frac{\dot{A}\dot{B}}{AB} + \frac{\dot{B}^2}{B^2} + \frac{w}{2}\phi^n\dot{\phi}^2 = \rho_{de} + \rho_m \tag{16}$$

$$\ddot{\phi} + \dot{\phi}\left(\frac{\dot{A}}{A} + 2\frac{\dot{B}}{B}\right) + \frac{n}{2}\frac{\dot{\phi}^2}{\phi} = 0. \tag{17}$$

$$\dot{\rho}_m + \left(\frac{\dot{A}}{A} + 2\frac{\dot{B}}{B}\right)\rho_m + \dot{\rho}_{de} + \left(\frac{\dot{A}}{A} + 2\frac{\dot{B}}{B}\right)(1+\omega_{de})\rho_{de} + 2\gamma\rho_\Lambda\frac{\dot{B}}{B} = 0, \quad (18)$$

where the overhead dot stands for ordinary differentiation with respect to time t.

The field equations (14)-(17) create a system of four differential equations with seven unknowns, namely, A, B, ρ_{de}, ρ_m, ω_{de}, γ and ϕ. As a result, to find an exact solution to the nonlinear equations, we assume a condition that the shear scalar is proportional to the scalar expansion, leading to a relation between the metric potentials as (Collins et al. 1980)

$$A = B^k \quad (19)$$

where $k \neq 1$ is a constant that preserves space-time's anisotropy. Thorne (1967) provides a reasonable description for this relationship and emphasizes its significance. Modern observations imply that Hubble's expansion of the universe is currently isotropic within $\approx$ 30% (Kristian and Sachs 1966; Kantowski and Sachs 1966), while redshift observations offer the range as $\frac{\sigma}{H} \leq 0.3$. Collins et al. (1980) determined that normal congruence follows this requirement ($\frac{\sigma}{H}$ is constant) for a spatially homogeneous metric.
Using Eq. (19) in Eqs. (14) and (15), we get

$$B^{k+1}\dot{B} = b_0\ exp\left(\int \frac{\gamma\rho_{de}B}{(1-k)\dot{B}}dt\right). \quad (20)$$

To obtain the explicit solution of the model, we assume (Adhav 2011; Santhi et al. 2016, 2017a; Aditya and Reddy 2018b)

$$\gamma = \frac{\gamma_0(1-k)\dot{B}}{B\rho_{de}} \quad (21)$$

where γ_0 is an arbitrary constant.
From Eqs. (20) and (21), we obtain the metric potentials as

$$A = \left[(k+2)\left(\frac{b_0}{\gamma_0}exp(\gamma_0 t) + b_1\right)\right]^{\frac{k}{k+2}};\ \ B = \left[(k+2)\left(\frac{b_0}{\gamma_0}exp(\gamma_0 t) + b_1\right)\right]^{\frac{1}{k+2}} \quad (22)$$

where b_0 and b_1 are integrating constants. Using Eq. (22) in Eq. (17), we obtain the scalar field as

$$\phi = \left[\frac{(n+2)\phi_0}{2b_1\gamma_0(k+2)}log\left(\frac{b_0}{\gamma_0} + b_1 exp(-\gamma_0 t)\right)\right]^{\frac{2}{n+2}}. \quad (23)$$

Using Eq. (22) the metric (6) can, now, be written as

$$ds^2 = dt^2 - \left[(k+2)\left(\frac{b_0}{\gamma_0}exp(\gamma_0 t) + b_1\right)\right]^{\frac{2k}{k+2}}dx^2 - \left[(k+2)\left(\frac{b_0}{\gamma_0}exp(\gamma_0 t) + b_1\right)\right]^{\frac{2}{k+2}}[dy^2 + dz^2] \quad (24)$$

The mean Hubble parameter can be obtained as

$$H=\frac{1}{3}\left(\frac{\dot{A}}{A}+2\frac{\dot{B}}{B}\right)=\frac{b_0 exp(\gamma_0 t)}{3\left(\frac{b_0}{\gamma_0}exp(\gamma_0 t)+b_1\right)}. \tag{25}$$

Rényi holographic dark energy: We consider a system with n, states with probability distribution P_i and satisfies the condition $\Sigma_{i=1}^{n}P_i=1$, Tsallis entropy is defined as (Tsallis 1988)

$$\mathcal{S}_{\mathcal{T}}=\frac{1}{\delta}\Sigma_{i=1}^{n}(P_i^{1-\delta}-P_i) \tag{26}$$

$\delta=1-U$, where, U is a real parameter which may be originated from the non-extensive features of system such as the long range nature of gravity. In addition, there is another Q-generalized entropy definition as

$$\mathcal{S}_{\mathcal{R}}=\frac{1}{\delta}ln\Sigma_{i=1}^{n}P_i^{1-\delta} \tag{27}$$

which returns to Rényi (1970). One can combine Eqs. (26) and (27) with each other to reach the relationship between Tsallis and Renyi entropies as (Komatsu 2017; Moradpour et al. 2017, 2018b)

$$\mathcal{S}_{\mathcal{R}}=\frac{1}{\delta}\ ln(1+\delta\mathcal{S}_{\mathcal{T}}). \tag{28}$$

$\mathcal{S}_{\mathcal{T}}=\frac{\mathcal{A}}{4}$. Here $\mathcal{A}=4\pi L^2$ and L is the IR cutoff, is the Bekenstein entropy and $T=(4\pi L)^{-1}$ is the Hawking temperature and d is a constant. We can determine the RHDE density using the relation $\rho_{de}dV\propto T\ dS$ as

$$\rho_{de}=\frac{3d^2}{L^2}(1+\pi\delta L^2)^{-1}. \tag{29}$$

Here we assume the RHDE model with the Hubble horizon cutoff $L=H^{-1}$. We find the Hubble cutoff by inserting it into Eq. (29) as

$$\rho_{de}=\frac{3d^2H^2}{1+\pi\delta H^{-2}}. \tag{30}$$

The fractional energy densities of matter (Ω_m) and DE (Ω_{de}) are given as

$$\Omega_m=\frac{\rho_m}{\rho_{cr}}=\frac{\rho_m}{3H^2}\quad and\quad \Omega_{de}=\frac{\rho_{de}}{\rho_{cr}}=\frac{d^2}{1+\pi\delta H^{-2}}, \tag{31}$$

ρ_{cr} is the critical energy density. The non-interactive and interacting RHDE models are studied in the following sections, and the physical importance of various cosmological parameters is discussed.

2.1 Non-interacting model

We are considering non-interacting DE and matter in this case. As a result, we have from Eq. (12) that both of these are conserved individually

$$\dot{\rho}_m + 3H\rho_m = 0, \tag{32}$$

$$\dot{\rho}_{de} + 3H(1+\omega_{de})\rho_{de} + 18\frac{\gamma_0(1-k)H^2}{(k+2)^2} = 0. \tag{33}$$

Differentiating Eq. (30) with respect to time, we obtain

$$\dot{\rho}_{de} = \rho_{de}\left(\frac{4\dot{H}}{H} - \frac{2H\dot{H}}{H^2+\pi\delta}\right). \tag{34}$$

In view of Eqs. (25) and (34), from Eq. (33), we obtain the EoS parameter of RHDE as

$$\omega_{de} = -1 + \frac{2\dot{H}}{3(H^2+\pi\delta)} - \frac{4\dot{H}}{H^2} - \frac{2\gamma_0(1-k)}{(k+2)^2 H\Omega_{de}} \tag{35}$$

where

$$\dot{H} = \frac{-b_0^2\ exp(2\gamma_0\ t)}{3\left(\frac{b_0}{\gamma_0}exp(\gamma_0 t) + b_1\right)^2} + \frac{b_0\ \gamma_0\ exp(\gamma_0\ t)}{3\left(\frac{b_0}{\gamma_0}exp(\gamma_0 t) + b_1\right)}. \tag{36}$$

Here Hubble parameter $H(t)$ and fractional energy density of RHDE Ω_{de} are respectively given in Eqs. (25) and (31).

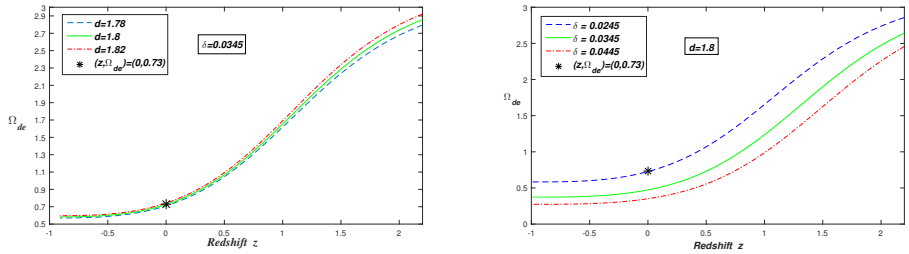

Fig. 1. Plot of DE energy density parameter Ω_{de} versus redshift z for $\gamma_0 = 0.3$, $b_0 = 0.018$ and $b_1 = -0.03$.

RHDE energy density parameter Ω_{de}*:* Fig. 1 depicts the behaviour of the density parameter Ω_{de} in terms of redshift z for various values of parameter d. Also, we assumed constant values ($k = 0.95$, $\gamma_0 = 0.3$, $b_0 = 0.018$, $d = 1.8$, $b_1 = -0.03$, $n = -1.5$ and $w = 10$) here, so that the energy density parameter Ω_{de} approaches 0.73 at the current era. Hinshaw et al. (2013) have investigated observational constraints on the total density parameter of DE Ω_{de} based on the final nine-year WMAP data in conjunction with additional cosmological data sets such as CMB and BAO, as

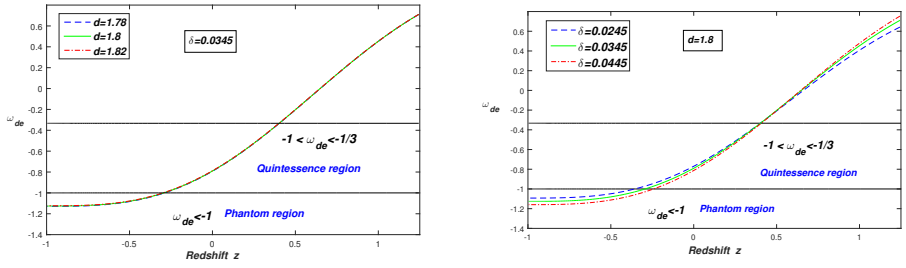

Fig. 2. Plot of EoS parameter ω_{de} versus redshift z for k= 0.95, γ_0= 0.3, b_0= 0.018 and b_1= − 0.03.

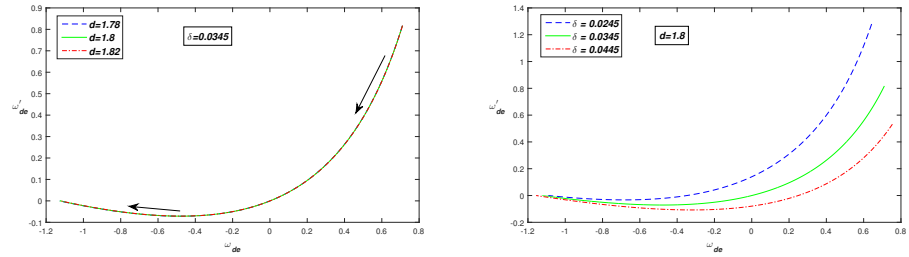

Fig. 3. Plot of $\omega_{de} - \omega'_{de}$ plane for k= 0.95, γ_0= 0.3, b_0= 0.018 and b_1= − 0.03.

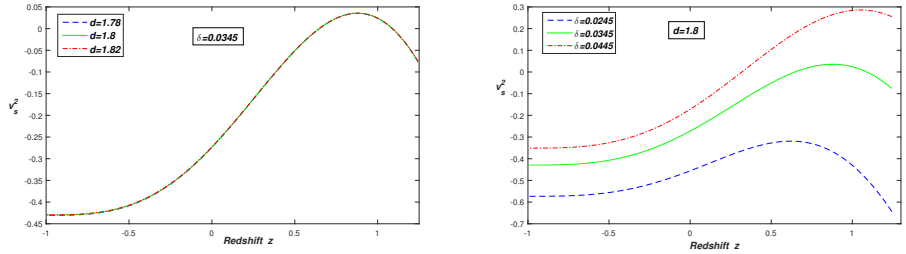

Fig. 4. Plot of v_s^2 versus redshift z for k= 0.95, γ_0= 0.3, b_0= 0.018 and b_1= − 0.03.

- Ω_{de}= 0.721 ± 0.025 (WMAP)
- Ω_{de}= 0.728 ± 0.019 (WMAP+eCMB)
- Ω_{de}= 0.707 ± 0.010 (WMAP+eCMB+BAO)
- Ω_{de}= 0.740 ± 0.015 (WMAP+eCMB+H0)
- Ω_{de}= $0.7135^{+0.0095}_{-0.0096}$ (WMAP+eCMB+BAO+H0).

At a 68% confidence level, Ade et al. (2014) established the following limits on the DE density parameter Ω_{de}= $0.717^{+0.028}_{-0.024}$ (WMAP-9) and Ω_{de}= $0.717^{+0.023}_{-0.020}$ (Planck+WP) by suggesting alternative combinations of observational approaches. As shown in Fig. 1, the RHDE density parameter Ω_{de} also meets the previously mentioned constraints, demonstrating the unified nature of our

results.

EoS parameter ω_{de}*:* The fluid EoS parameter connects its pressure p and energy density ρ by the relation, $\omega=\frac{p}{\rho}$. Different EoS values correlate to distinct eras of the universe in its early decelerating and current accelerating expansion phases. For $\omega=\frac{1}{3}$, $\omega=1$ and $\omega=0$ (decelerating phases), it contains radiation, stiff fluid and matter-dominated (dust), respectively. It symbolizes the quintessence for $-1<\omega<-1/3$, the cosmological constant for $\omega=-1$, and the phantom for $\omega<-1$. Fig. 2 depicts the behaviour equation of the non-interacting model's EoS parameter in terms of redshift for different values of d and δ. It can be observed that initially the model begins in the matter-dominated era, varies in the quintessence epoch, and eventually approaches the phantom epoch by crossing the phantom divided line ($\omega_{de}=-1$). This behaviour is commonly known as the quintom-like nature. Furthermore, as the parameter δ increases, the model evolves with high phantom values. The present value (at $z=0$) of the EoS parameter of our obtained model $(z,\omega_{de})=(0,-0.81)$ is in good agreement with recent Planck data (Aghanim et al. 2020).

$\omega_{de}-\omega'_{de}$ *plane:* Here, the behaviour of $\omega_{de}-\omega'_{de}$ (where prime respresents the derivative with regard to '$ln(a\,(t))$') plane is presented. This plane was initially suggested to investigate the evolution of the quintessence DE (Caldwell and Linder 2005). This plane can be divided into two portions, which are referred to as freezing ($\omega_{de}<0$, $\omega'_{de}<0$) and thawing ($\omega_{de}<0$, $\omega'_{de}>0$). By taking the derivative of Eq. (35) with regard to $ln(a\,(t))$, we obtain

$$\omega'_{de}=\frac{6\ddot{H}(H^2+\pi\delta)+12\dot{H}^2H}{9H(H^2+\pi\delta)^2}-\frac{4}{3}\left[\frac{\ddot{H}}{H^2}-\frac{2\dot{H}^2}{H^3}\right]+\frac{2\gamma_0(1-k)}{(k+2)^2}\left[\frac{\dot{H}}{H^2\Omega_{de}}+\frac{\dot{\Omega}_{de}}{\Omega_{de}H}\right], \tag{37}$$

where

$$\ddot{H}=\frac{2b_0^3\ exp(3\gamma_0\ t)}{3\left(\frac{b_0}{\gamma_0}exp(\gamma_0 t)+b_1\right)^3}-\frac{b_0^2\ \gamma_0\ exp(2\gamma_0\ t)}{\left(\frac{b_0}{\gamma_0}exp(\gamma_0 t)+b_1\right)^2}+\frac{b_0\ \gamma_0^2\ exp(\gamma_0\ t)}{3\left(\frac{b_0}{\gamma_0}exp(\gamma_0 t)+b_1\right)} \tag{38}$$

and

$$\dot{\Omega}_{de}=\frac{2H\dot{H}\pi\delta d^2}{(H^2+\pi d)^2}. \tag{39}$$

We plotted the behaviour of the $\omega_{de}-\omega'_{de}$ plane for our non-interacting RHDE model for different values in Fig. 3. Our non-interacting RHDE model initially starts from the thawing region and varies in the freezing region at the present epoch. Modern cosmological observations support that the freezing region unveils a higher cosmic acceleration era than the thawing region. Hence, our

model exhibits cosmic acceleration in the freezing region and good agreement with the observations.

Squared sound speed v_s^2*:* This parameter v_s^2 is used to investigate the model's stability. If $v_s^2 > 0$, we get a stable model; otherwise ($v_s^2 < 0$), one can get an unstable model. Here, v_s^2 has the following form:

$$\begin{aligned} v_s^2 &= \frac{\dot{p}_{de}}{\dot{\rho}_{de}} = \omega_{de} + \dot{\omega}_{de}\frac{\rho_{de}}{\dot{\rho}_{de}} \\ &= -1 + \frac{2\dot{H}}{3(H^2+\pi\delta)} - \frac{4\dot{H}}{H^2} - \frac{2\gamma_0(1-k)}{(k+2)^2 H\Omega_{de}} + \left\{ \frac{6\ddot{H}(H^2+\pi\delta) + 12\dot{H}^2 H}{9(H^2+\pi\delta)^2} \right. \\ &\quad \left. -\frac{4}{3}\left[\frac{\ddot{H}}{H} - \frac{2\dot{H}^2}{H^2}\right] + \frac{2\gamma_0(1-k)}{(k+2)^2}\left[\frac{\dot{H}}{H\Omega_{de}} + \frac{\dot{\Omega}_{de}}{\Omega_{de}}\right] \right\} \\ &\quad \times \left(\frac{H(H^2+\pi\delta)}{4\dot{H}(H^2+\pi\delta-2H^2\dot{H})}\right) \end{aligned} \tag{40}$$

Fig. 4 exhibits the behaviour of v_s^2 versus redshift. We notice that v_s^2 is initially positive, implying that our model is unstable. Furthermore, as the universe evolves, $v_s^2 < 0$ demonstrates model instability. It should be noted that several authors in the literature (Myung 2007; Jawad et al. 2013; Jawad and Chattopadhyay 2015) have done stability analysis of DE models in several gravitational theories, where they have similarly obtained unstable behaviour of the DE models.

2.2 Interacting model

Here, we presume that DE and matter interact with one another. As a result, the energy-conservation equation Eq. (18) can be written for matter and DE as

$$\dot{\rho}_m + 3H\rho_m = Q, \tag{41}$$

$$\dot{\rho}_{de} + 3H(1+\omega_{de})\rho_{de} + 18\frac{\gamma_0(1-k)H^2}{(k+2)^2} = -Q. \tag{42}$$

Here Q is assumed as follows

$$Q = 3\beta q H \rho_{de} \tag{43}$$

where Q is the matter-DE interaction term and is a coupling constant (Xu 2020; Sobhanbabu and Santhi 2021). Because the positive parameter β will result in negative ρ_m in the flat universe, the parameter β is assumed to be negative. Q can shift its sign from $Q < 0$ to $Q > 0$ as the universe's expansion changes from deceleration ($q > 0$) to acceleration ($q < 0$). For $Q < 0$, energy moves from matter to RHDE, whereas for $Q > 0$, energy flows from RHDE to matter.

Using Eqs. (25) and (34) in Eq. (42), we obtain the EoS parameter as

$$\omega_{de}=-1-\beta q+\frac{2\dot{H}}{3(H^2+\pi\delta)}-\frac{4\dot{H}}{H^2}-\frac{2\gamma_0(1-k)}{(k+2)^2H\Omega_{de}} \tag{44}$$

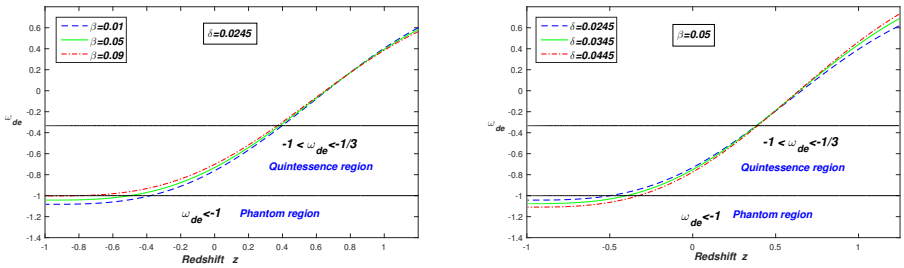

Fig. 5. Plot of EoS parameter ω_{de} versus redshift z for $\gamma_0=0.3$, $d=1.8$, $b_0=0.018$ and $b_1=-0.03$.

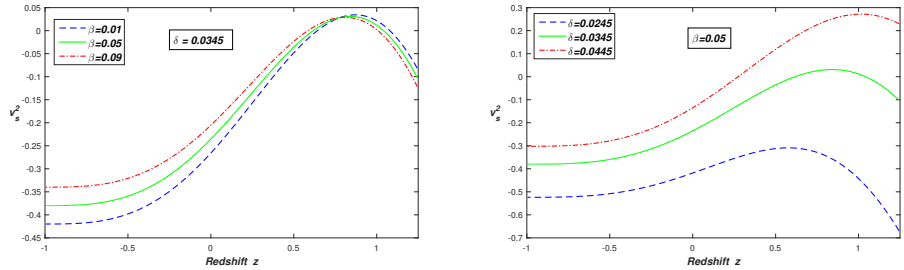

Fig. 6. Plot of v_s^2 versus redshift z for $k=0.95$, $\gamma_0=0.3$, $d=1.8$, $b_0=0.018$ and $b_1=-0.03$.

Equation of state parameter ω_{de}*:* Fig. 5 depicts the behavior of our non-interacting model's EoS parameter for various values of δ and β. This model originates in the matter-dominated epoch, fluctuates in the quintessence era, and eventually reaches the phantom epoch by crossing the phantom divided line ($\omega_{de}=-1$). This is referred to as the universe's quintom-like nature. Furthermore, as β grows, the model progresses with high phantom values, whereas the EoS parameter increases, and the model becomes more oriented towards the ΛCDM model. Furthermore, the current value of our non-interacting model's EoS parameter $(z,\omega_{de})=(0,-0.83)$ is in agreement with modern Planck data (Aghanim et al. 2020).

$\omega_{de} - \omega'_{de}$ *plane:* We get ω'_{de} by taking the differentiating of Eq. (44) with regard to $ln(a\,(t))$, which is the same as Eq. (37). As a result, the behaviour of our non-interacting model from the $\omega_{de} - \omega'_{de}$ plane is very similar to that of the interacting model (ref. Fig. 3).

Squared sound speed v_s^2*:* This parameter v_s^2, in this case, can be obtained as

$$v_s^2 = -1 - \beta\ q + \frac{2\dot{H}}{3(H^2+\pi\delta)} - \frac{4\dot{H}}{H^2} - \frac{2\gamma_0(1-k)}{(k+2)^2 H\Omega_{de}} + \{\frac{6\ddot{H}(H^2+\pi\delta)+12\dot{H}^2H}{9(H^2+\pi\delta)^2}$$

$$-\frac{4}{3}\left[\frac{\ddot{H}}{H} - \frac{2\dot{H}^2}{H^2}\right] + \frac{2\gamma_0(1-k)}{(k+2)^2}\left[\frac{\dot{H}}{H\Omega_{de}} + \frac{\dot{\Omega}_{de}}{\Omega_{de}}\right]\}\left(\frac{H(H^2+\pi\delta)}{4\dot{H}(H^2+\pi\delta-2H^2\dot{H})}\right) \tag{45}$$

Figure 6 depicts the behaviour of v_s^2 in terms of redshift z. Initially $v_s^2 > 0$ for high values $\delta = 0.0445$ indicating a stable model, and for $z \leq 0.5$ the squared sound speed $v_s^2 < 0$ indicating that the model is unstable at late times. The examination of DE models in several alternative theories of gravity in the literature (Myung 2007; Jawad et al. 2013; Jawad and Chattopadhyay 2015) demonstrates this behaviour of the model.

Scalar field $\phi(t)$: Eq. (23) gives the scalar field of the models, and Fig. 7 exhibits the behaviour of the $\phi(t)$ in terms of redshift for different values of b_1. The scalar field decreases as the cosmos evolves, as shown in Fig. 7. As the scalar field diminishes, so does the related kinetic energy. According to the literature, Raju et al. (2020a, 2020b) analyzed the anisotropic DE and cosmic string cosmological model with a massive scalar field and discovered that the scalar field decreases as cosmic time increases. Aditya et al. (2022) discussed the BT-IX DE model in Lyra geometry with a massive scalar meson field. Rao et al. (2021, 2022) studied BT-I and BT-II massive scalar field models and discovered that the scalar field is a decreasing function. The above discussion concluded that the study of our scalar field is similar to the above-discussed DE models.

Energy conditions: The study of energy conditions was initiated by the Raychaudhuri equations, which are crucial in any consideration of the congruence of null and time-like geodesics. Other broad theorems about how strong gravitational fields behave are illustrated using the energy conditions. The typical energy scenarios are as follows:

- Dominant energy condition (DEC): $\rho_{de} \geq 0$, $\rho_{de} \pm p_{de} \geq 0$,
- Strong energy conditions (SEC) : $\rho_{de} + p_{de} \geq 0$, $\rho_{de} + 3p_{de} \geq 0$,
- Null energy conditions (NEC): $\rho_{de} + p_{de} \geq 0$,
- Weak energy conditions (WEC): $\rho_{de} \geq 0$, $\rho_{de} + p_{de} \geq 0$.

Fig. 8 depicts the energy conditions for various values of parameter d for our RHDE models. It is clear that the NEC are violated, and the model results in a Big Rip. It can also be seen that the WEC meets the requirement $\rho_{de} \geq 0$. In

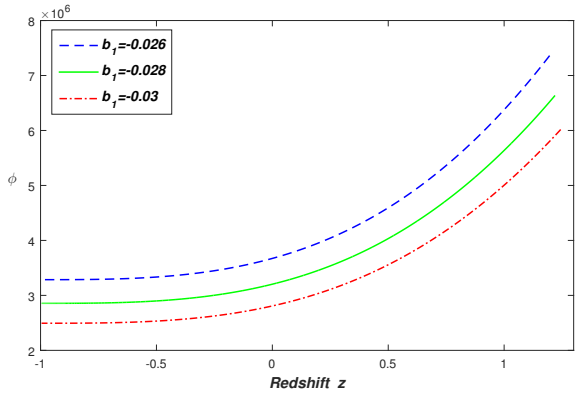

Fig. 7. Plot of scalar field ϕ versus redshift z for k= 0.95, γ_0= 0.3, b_0= 0.018 and n= − 1.5.

addition, Fig. 8 shows that the DEC $\rho_{de}+p_{de}$ is not satisfied. Additionally, our models violate the SEC, which is appropriate. This tendency, which is caused by the universe's late-time acceleration, is consistent with recent observational data.

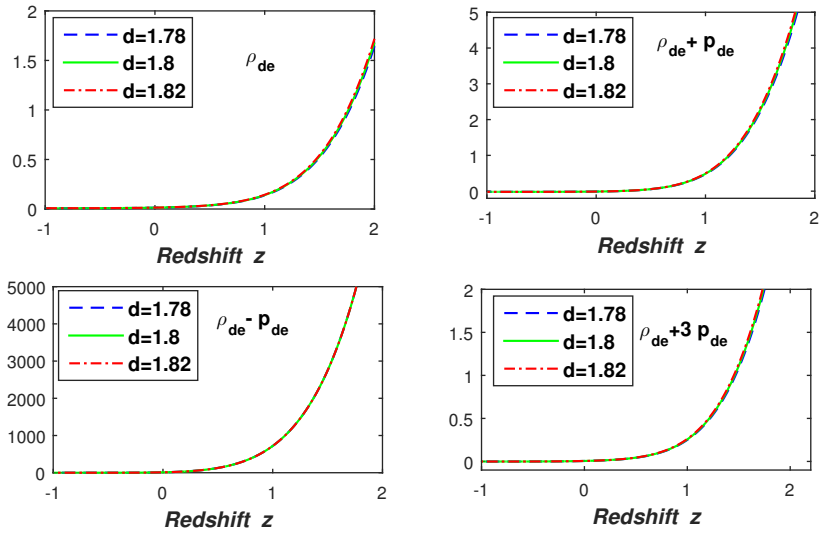

Fig. 8. Plot of energy conditions versus redshift z for k= 0.95, γ_0= 0.3 and b_0= 0.018. b_1= − 0.03 and n= − 1.5.

Deceleration parameter: The deceleration parameter's (q) signature indicates whether the model accelerates or decelerates. If $q> 0$, the model exhibits decelerating expansion, constant expansion if $q= 0$, and accelerating scenario if $-1 \leq q< 0$. For $q= -1$, the universe shows de Sitter (exponential) expansion, and for $q<-1$, it exhibits super-exponential expansion. In both scenarios (interacting and non-interacting), the deceleration parameter for our model is provided by

$$q= -1 - \frac{\dot{H}}{H^2} = -1 - \frac{b_1\gamma_0}{b_0\ exp(\gamma_0\ t)} \tag{46}$$

Figure 9 depicts the behavior of the deceleration parameter in terms redshift z for different b_1 values. It should be emphasized that both models indicate a smooth evolution from the universe's early decelerated phase to its current accelerated phase. In this region $0.65 <z< 0.8$, the universe changed from a decelerating to an accelerating phase. This is consistent with recent observations in cosmology (Capozziello et al. 2014; Muthukrishna and Parkinson 2016). Capozziello et al. (2014) investigated cosmographic limitations on the cosmic deceleration-acceleration transition redshift in $f(R)$ theory of gravity and discovered that the accelerating expansion's transition redshift (z_t) is provided by $0.3 <z_t< 0.8$. Muthukrishna and Parkinson (2016) investigated cosmographic evaluation of the transition to acceleration using SN-Ia and BAO and obtained boundaries on the transition redshift for the various expansions, finding $z_{acc}> 0.14$ at 95% confidence in the most conservative case.

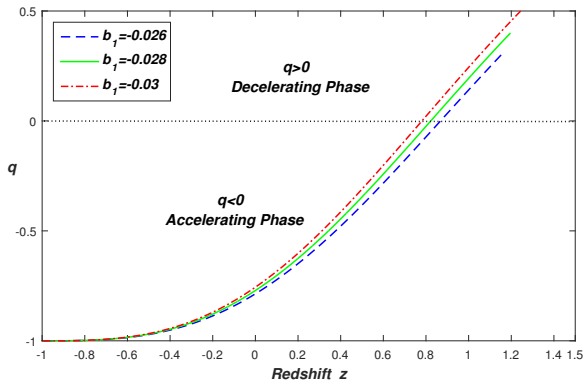

Fig. 9. Plot of deceleration parameter q versus redshift z for $k= 0.95$, $\gamma_0= 0.3$ and $b_0= 0.018$.

Statefinder parameters: In recent years, a number of DE models have been put out to explain the universe's accelerated expansion. These multiple DE models' Hubble and deceleration parameters all have the same present value, making it impossible for them to distinguish between the DE models. In order to accomplish this, Sahni et al. (2003) combined the deceleration and Hubble

parameters, which are written as

$$r=\frac{\dddot{a}}{aH^3}, \quad s=\frac{r-1}{3(q-1/2)} \tag{47}$$

The regions shown below are defined by these statefinders: ΛCDM for $(r,s)=(1,0)$ and CDM model for $(r,s)=(1,1)$; $r<1$ gives quintessence and $s>0$ gives phantom DE phases; $r>1$ with $s<0$ establishes the Chaplygin gas model.
The statefinder parameter for our models are

$$r = 10 - \frac{18\gamma_0}{b_0\ exp(\gamma_0 t)}\left(\frac{b_0}{\gamma_0}exp(\gamma_0 t)+b_1\right) + \frac{9\gamma_0^2}{b_0^2\ exp(2\gamma_0 t)}\left(\frac{b_0}{\gamma_0}exp(\gamma_0 t)+b_1\right)^2 \tag{48}$$

$$s = \left[3 - \frac{6\gamma_0}{b_0\ exp(\gamma_0 t)}\left(\frac{b_0}{\gamma_0}exp(\gamma_0 t)+b_1\right) + \frac{3\gamma_0^2}{b_0^2\ exp(2\gamma_0 t)}\left(\frac{b_0}{\gamma_0}exp(\gamma_0 t)+b_1\right)^2\right] \times\left(-\frac{3}{2}-\frac{b_1\gamma_0}{b_0\ exp(\gamma_0\ t)}\right) \tag{49}$$

Figure 10 depicts the $r-s$ plane's trajectory. The $r-s$ plane resembles the ΛCDM model at late times. It can be seen that the behaviour of the $r-s$ plane is similar to that of dynamical DE models such as Chaplygin gas ($s<0$ and $r>1$).

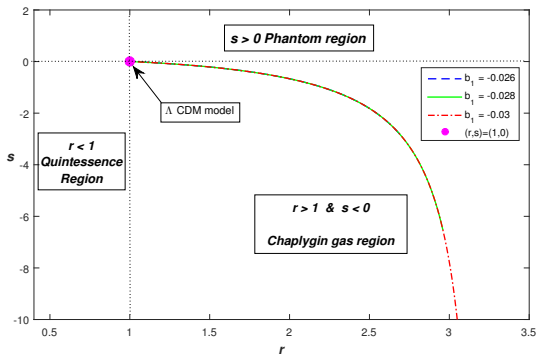

Fig. 10. Plot of statefinders for $k=0.95$, $\gamma_0=0.3$ and $b_0=0.018$.

***r*−*q* plane:** Figure 11 depicts the development of our models in the $r-q$ plane. The values $(r,q)=(1,0.5)$ represents standard cold dark matter (SCDM) whereas $(r,q)=(1,-1)$ represents the steady state (SS) model. The ΛCDM model evolves along the dotted line (see Fig. 11) from a fixed point in the SCDM model to a fixed point in the SS model. At late times, our model comes close to the SS model. Aditya et al. (2022) and Singh and Kumar (2016) examined the $r-q$ plane analysis of the DE model in the presence of a massive

scalar meson field and HDE model with constant bulk viscosity. The $r - q$ trajectory of our model is found to be quite comparable to the DE models previously presented in the literature (Aditya et al. 2022; Singh and Kumar 2016).

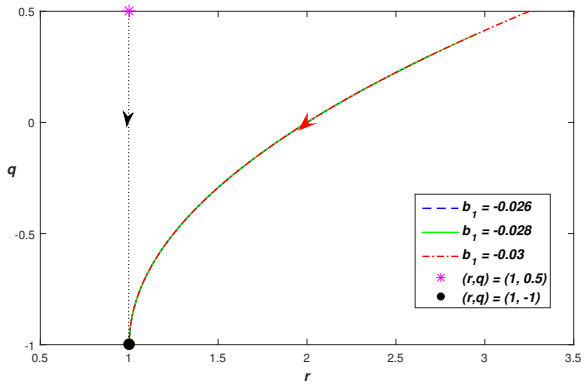

Fig. 11. Plot of the $r - q$ plane for k= 0.95, γ_0= 0.3 and b_0= 0.018.

3 Discussion and Final Remarks

There have been some interesting studies on the accelerating expansion of the universe. There are two approaches put out to explain this cosmic acceleration. Studying numerous dynamical DE models is one method while taking into account alternate theories of gravitation is another method. Here, using the SB theory of gravity (1986), we investigated the accelerated expansion while assuming RHDE in the LRS Bianchi type-I universe. By utilizing the relationship between the metric potentials, we have obtained a solution to the SB field equations, which yields a variable deceleration parameter. We have thought about scenarios of matter and DE that interact and do not interact. We investigated several cosmological parameters to assess the validity of these results. Our findings are as follows:

– The total RHDE density parameter Ω_{de} decreases as the universe evolves (Fig. 1). We selected the fixed values (k= 0.95, γ_0= 0.3, b_0= 0.018, d=1.8 and b_1= − 0.03) so that we arrive at the energy density parameter Ω_{de} approaching 0.73 at the present epoch. It can be concluded that the RHDE density parameter Ω_{de} meets the observational limits from WMAP, Planck data, and BAO (Hinshaw et al. 2013; Ade et al. 2014). As the universe evolves, the scalar field of our models decreases (Fig. 7). We can see that as the scalar field decreases, so does the associated kinetic energy increase. According to the literature (Raju et al. 2020a, 2020b; Aditya et al. 2022; Rao et al. 2021, 2022), the study of our scalar field is very similar to the previously mentioned dark energy models. The NEC is violated, and

hence the model results in a Big Rip (Fig. 8). The WEC satisfied $\rho_{de} \geq 0$, however, the DEC $\rho_{de} + p_{de}$ did not satisfy. Additionally, as should be the case, our model violates the SEC. This tendency, which is caused by the universe's late-time acceleration, is consistent with recent observational data.

- The $\omega_{de} - \omega'_{de}$ plane for our RHDE models (similar to non-interactive and interacting models) is shown in Fig. 3, and the trajectories meet both freezing and thawing zones. However, in the present and the future, the models only show freezing regions. Recent observations confirm that models that differ in the freezing area are the best candidates for explaining cosmic acceleration. This plane's trajectories are also consistent with observational data (Ade et al. 2014) $\omega_{de}{=}-1.13^{+0.24}_{-0.25}$, $\omega'_{de}{<}\ 1.32$ $(Planck{+}WP{+}BAO)$. The stability analysis shows that the models (ref. Figs. 4 and 6) are stable in the past but unstable in the present and future eras. Our models' stability analysis is very comparable to that of RHDE models in the literature (Bhattacharjee 2020; Prasanthi and Aditya 2021).
- For adequate parameter values, the deceleration parameter undergoes signature flipping. So, the models demonstrate a smooth transition from the early decelerated phase to the present accelerated phase of the universe. The transition redshift of the universe (Fig. 9) at $0.65 {<} z {<}\ 0.8$. At a 95% confidence level, this is in agreement with SN-Ia and BAO cosmological observations.
- At late times, the statefinder plane $(r - s)$ corresponds to the ΛCDM model, and its behaviour is identical to that of the dynamical DE model, such as Chaplygin gas ($s{<}\ 0$ and $r{>}\ 1$) (Fig. 10). At late times, the model approaches the SS model ($r - q$ plane and Fig. 11). The $r - q$ trajectory of our model is found to be quite similar to the DE models in the literature (Aditya et al. 2022; Singh and Kumar 2016).

In this section, we give comparisons of our results with current research on this topic and with observational data.

Sadri and Vakili (2018) investigated the new HDE model in the context of the BD theory of gravity. They have identified an EoS parameter capable of reaching the phantom era $\omega_{de}{<}-1$ without the need for interaction between dark sectors. Sharif et al. (2018) examined BT-I NHDE models in the BD theory of gravity and obtained the EoS parameter, which leads to an accelerated expansion of the universe. Aditya and Reddy (2018a) used the SB theory of gravity to investigate new HDE in the BT-I universe. They constructed interacting and non-interactive DE models and discovered that the interacting model approaches the ΛCDM model, whereas the non-interacting model marks the phantom division line and attains a constant value in the phantom region. In the framework of the SB theory of gravity, Santhi and Sobhanbabu (2020) discussed the BT-III universe with THDE and the models demonstrate quintom behaviour. Sobhanbabu and Santhi (2021) examined the Kantowski-Sachs THDE model with interaction and discovered quintom behaviour. Sharma and Dubey (2022) explored the RHDE model in the context of a flat FRW Universe using three distinct parametrizations of the interaction term and discovered that two models change only in the phantom area and one model just in the quintessence region. Bhattacharjee (2020) discussed how THDE and RHDE models interact with hybrid expansion laws. According to

his results, the Tsallis HDE model varies in the quintessence zone and will approach the phantom divide line in the future, but the RHDE model fluctuates in the phantom region.

Examination of the EoS parameters reveals that the anisotropic RHDE models (both interacting and non-interacting) start in the material-dominated zone, cross the phantom dividing line, and reach a constant value in the phantom region. This is similar to and unlike the various models outlined above. In particular, as the β increases, the model approaches the ΛCDM model in the near future. Furthermore, it is useful to show here that the current values of the EoS parameter value in our model $\omega_{de} \approx -0.92$ are in good agreement with Planck's observed data (Aghanim et al. 2020)
$\omega_{de} = -1.56^{+0.60}_{-0.48}$ $(Planck + TT + lowE)$;
$\omega_{de} = -1.58^{+0.52}_{-0.41}$ $(Planck + TT, TE, EE + lowE)$;
$\omega_{de} = -1.57^{+0.50}_{-0.40}$ $Planck + TT, TE, EE + lowE + lensing)$;
$\omega_{de} = -1.04^{+0.10}_{-0.10}$ $(Planck + TT, TE, EE + lowE + lensing + BAO)$.
It demonstrates the agreement of our findings with the cosmic evidence presented above. According to the comparison above, our RHDE models are more viable in the SB theory of gravity. At $0.65 < z < 0.8$, the universe transitioned from the decelerating to the accelerating phase. This is consistent with recent observations in cosmology. Furthermore, the current value of the deceleration parameter $q(t)$ for our models is $q \approx -0.8$, which is consistent with the modern observations (Capozziello et al. 2019; Amirhaschchi and Amirhaschchi 2019) given as $q = -0.930 \pm 0.218$ $(BAO + Masers + TDSL + Pantheon + H_z)$. Finally, we briefly summarize our results as follows:

- The deceleration parameters show transitions from previous deceleration epochs to the current cosmic acceleration, which is consistent with current observations.
- When compared to recent measurements, the EoS parameter displays quintom behaviour and consistent ranges.
- $\omega_{de} - \omega'_{de}$ plane shows a freezing region within the observational range.
- The model is stable in the past, but unstable in the current and future epochs.
- The statefinder parameters meet the Chaplygin gas behaviour and the ΛCDM limit.
- Eventually, the model approaches a stationary model, as shown in the $r-q$ plane.

Acknowledgments: I am grateful to the anonymous reviewer for constructive comments which have improved the presentation of the work. The work has been supported financially by National Board for Higher Mathematics, Department of Atomic Energy, Govt. of India under the Research project No.: 02011/8/2023 NBHM(R.P.)/R & D II/3073.

References

Ade, P.A.R., et al., 2014, *[Plancks Collaboration] A&A, 571, A16*
Adhav, K.S., 2011, *Int. J. Astron. Astrophys., 1, 204*
Aditya, Y., 2023, *Bulgarian Astronomical Journal, 39, 12-27*

Aditya, Y., et al., 2019, *Eur. Phys. J. C 79, 1020*
Aditya, Y., et al., 2022, *Int. J. Mod. Phys. A, 37(16), 2250107*
Aditya, Y., Prasanthi, U.Y.D., 2023, *Bulgarian Astronomical Journal, 38, 52*
Aditya, Y., Reddy, D.R.K., 2018a, *Astrophys. Space Sci., 363, 207*
Aditya, Y., Reddy, D.R.K., 2018b, *Int. J. Geom. Methods Mod. Phys., 15, 1850156*
Aghanim, N., et al., 2020, *[Plancks Collaboration] A&A, 641, A6*
Bamba, K., et al., 2012, *Astrophys. Space Sci., 341, 155*
Bento, M.C., et al., 2002, *Phys. Rev. D, 66, 043507*
Bhattacharjee, S., 2020, *Astrophys. Space Sci., 365, 103*
Brans, C., Dicke, R.H., 1961, *Phys. Rev., 124, 925*
Cai, R.G., 2007, *Phys. Lett. B, 657, 228*
Caldwell, R.R., 2002, *Phys. Lett. B, 545, 23*
Caldwell, R.R., Linder, E.V., 2005, *Phys. Rev. Lett., 95, 141301*
Capozziello, S., et al., 2014, *Phys. Rev. D, 90, 044016*
Capozziello, S., et al., 2019, *MNRAS, 484, 4484*
Chunlen, S., Rangdee, P., 2021, *Phayao Research Conference 10, 2413*
Clifton, T., et al., 2012, *Phys. Rep., 513, 1*
Cohen, A., Kaplan, D., Nelson, A., 1999. *Phys. Rev. Lett., 82, 4971*
Collins, C.B., et al., 1980, *Gen. Relativ. Gravit., 12, 805*
Copeland, E.J., et al., 2006, *Int. J. Mod. Phys. D, 15, 1753*
Harko, T., et al., 2011, *Phys. Rev. D, 84, 024020*
Hinshaw, G., et al., 2013, *ApJS, 208, 19*
Hooft, G.T., gr-qc/9310026 (1993)
Hsu, S.D.H., 2004, *Phys. Lett. B, 594, 13*
Iqbal, A., Jawad, A., 2019, *Physics of the Dark Universe, 26, 100349*
Jahromi, A.S., et al., 2018, *Phys. Lett. B, 780, 21*
Jawad, A., Chattopadhyay, S., 2015, *Astrophys. Space Sci., 357, 37*
Jawad, A., et al., 2013, *Astrophys. Space Sci., 344, 489*
Kamenshchik, A.Y., et al., 2001, *Phys. Lett. B, 511, 265*
Kantowski, R., Sachs, R.K., 1966, *J. Math. Phys., 7, 433*
Komatsu, N., 2017, *Eur. Phys. J. C, 77, 229*
Kristian, J., Sachs, R.K., 1966, *Astrophys. J., 143, 379*
Maity, S., Debnath, U., 2019, *Eur. Phys. J. Plus, 134, 514*
Mishra, B., et al., 2018, *Astrophys. Space Sci., 363, 86*
Moradpour, H., et al., 2017, *Phys. Rev. D, 96, 123504*
Moradpour, H., et al., 2018a, *Phys. Lett. B, 783, 82*
Moradpour, H., et al., 2018b, *Eur. Phys. J. C, 78, 829*
Muthukrishna, D., Parkinson, D., 2016, *JCAP, 11, 052*
Myung, Y.S., 2007, *Phys. Lett. B, 652, 223*
Nojiri, S., et al., 2017, *Phys. Rep., 692, 1*
Nojiri, S., Odintsov, S.D., 2003a, *Phys. Rev. D, 562, 147*
Nojiri, S., Odintsov, S.D., 2003b, *Phys. Rev. D, 68 , 123512*
Padmanabhan, T., 2002, *Phys. Rev. D, 66, 02131*
Padmanabhan, T., 2008, *Gen. Relativ. Gravit., 40, 529*
Perlmutter, S, et al., 1999, *Astrophysical Journal, 517, 565-586*
Prasanthi, U.Y.D., Aditya, Y., 2020, *Results of Physics, 17, 103101*
Prasanthi, U.Y.D., Aditya, Y., 2021, *Physics of the Dark Universe, 31, 100782*
Quiros, I., Horta-Rangel, F.A., 2023, *Int.J.Mod.Phys.D, 32(06), 2350033*
Raju, K.D., et al., 2020a, *Can. J. Phys, 98, 993*
Raju, K.D., et al., 2020b, *Astrophys. Space Sci., 365, 28*
Rao, V.U.M., Prasanthi, U.Y.D., 2017, *Eur. Phys. J. Plus, 132, 64*
Rao, M.P.V.V.B., et al., 2021, *Int. J. Mod. Phys. A, 36(36), 2150260*
Rao, M.P.V.V.B., et al., 2022, *New Astr., 92, 101733*
Rényi, A., *Probability Theory, North-Holland, Amsterdam,* 1970
Riess, A G, et al. 1998, *Astron. J., 116, 1009–1038*
Sadri, E., Vakili, B., 2018, *Astrophys. Space Sci., 363, 13*
Saez, D., Ballester, V.J., 1986, *Phys. Lett. A, 113, 467*
Sahni, V., Shtanov, J., 2003, *J. Cosmol. Astropart. Phys., 11, 014*
Sahni, V., et al., 2003, *JETP Lett., 77, 201*
Santhi, M.V., et al. 2017a, *Int. J. Theor. Phys., 56, 362*
Santhi, M.V., et al., 2017b, *Can. J. Phys., 95, 179–183*
Santhi, M.V., Chinnappalanaidu, T., 2022, *New Astr., 92, 101725*

Santhi, M.V., Chinnappalanaidu, T., 2023, *Astrophys. Space Sci., 368 (4), 1-17*
Santhi, M.V., et al., 2016, *Astrophys. Space Sci., 361, 142*
Santhi, M.V., Sobhanbabu, Y., 2020, *Eur. Phys. J. C, 80, 1198*
Setare, M.R., 2007, *Phys. Lett. B, 653, 116*
Sharif, M., et al., 2018, *Symmetry, 10, 153*
Sharma, U.K., Dubey, V.Ch., 2022, *Int. J. Geom. Theories Mod. Phys., 19(1), 2250010*
Singh, C.P., Kumar, P., 2016, *Astrophys. Space Sci., 361, 157*
Sobhanbabu, Y., Santhi, M.V., 2021, *Eur. Phys. J. C, 81, 1040*
Spergel, D.N., et al., 2003, *Astrophys. J. Suppl. Ser., 148, 175*
Susskind, L., 1995, *J. Math. Phys., 36, 6377*
Tavayef, M., et al., 2018, *Phys. Lett. B., 781, 195*
Tegmark, M., et al., 2004, *Phys. Rev. D, 69, 103501.*
Thorne, K.S., 1967, *Astrophys. J., 148, 51*
Tsallis, C., 1988, *J. Stat. Phys., 52, 479*
Tsallis, C., Cirto, L.J.L., 2013, *Eur. Phys. J. C, 73, 2487*
Vinutha, T., et al., 2023, *Int. J. Geom. Theories Mod. Phys., 20(07), 2350119*
Xu, Y.D., 2020, *Commun. Theor. Phys, 72, 015402*
Younas, M., et al., 2019, *Advances in High Energy Physics, 2019, 1287932*